Am J Cancer Res 2022;12(7):3318-3332
www.ajcr.us /ISSN:2156-6976/ajcr0142490

Original Article

A novel 8-gene panel for prediction of early biochemical recurrence in patients with prostate cancer after radical prostatectomy

Jinan Guo[1,2*], Chenhui Zhao[3*], Xinzhou Zhang[4*], Zhong Wan[5*], Tingting Chen[6], Jiashun Miao[6], Jinping Cai[6], Wenchuan Xie[6], Hao Chen[6], Mengli Huang[6], Xiaochen Zhao[6], Wei Wei[7], Qi Shen[8]

[1]Department of Urology, The Second Clinical Medical College of Jinan University, Shenzhen People's Hospital, The First Affiliated Hospital of South University of Science and Technology of China, Shenzhen, China; [2]Shenzhen Urology Minimally Invasive Engineering Center, Shenzhen, China; [3]Ruijin Hospital Lu Wan Branch, Shanghai Jiao Tong University School of Medicine, Shanghai, China; [4]Department of Nephrology, Shenzhen key Laboratory of Kindey Diseases, The Second Clinical Medical College of Jinan University, Shenzhen People's Hospital, The First Affiliated Hospital of South University of Science and Technology of China, Shenzhen, China; [5]Shuguang Hospital, Shanghai University of Traditional Chinese Medicine, Shanghai, China; [6]3D Medicines, Inc, Shanghai, China; [7]Department of Urology, Hwa Mei Hospital, University of Chinese Academy of Sciences, Ningbo, China; [8]Department of Hematology, The Second Clinical Medical College of Jinan University, Shenzhen People's Hospital, The First Affiliated Hospital of South University of Science and Technology of China, Shenzhen, China. [*]Equal contributors.

Received February 22, 2022; Accepted April 14, 2022; Epub July 15, 2022; Published July 30, 2022

Abstract: Approximately 25% of prostate cancer (PCa) cases experience biochemical recurrence (BCR) following radical prostatectomy (RP). The patients with BCR, especially with BCR ≤2 year after RP (early BCR), are more likely to develop clinical metastasis and castration resistance. Now decision-making regarding BCR after RP relies solely on clinical parameters. We thus attempted to establish an early BCR-risk prediction model by combining a molecular signature with clinicopathological features for guiding clinical decision-making. In this study, an 8-gene signature was derived, and these eight genes were *SPTBN2*, *LGI3*, *TGM3*, *LENG9*, *HAS3*, *SLC25A27*, *PCDHGA1*, and *ADPRHL1*. The Kaplan-Meier analysis revealed a significantly prolonged BCR-free survival in the patients with low-risk scores compared to those with high-risk scores in both training and validation datasets. Harrell's concordance index and time-dependent receiver operating characteristic analysis demonstrated that this gene signature tended to outperform three commercial panels at early BCR prediction. Moreover, this signature was also proven as an independent predictor of BCR-free survival. A nomogram, incorporating the gene signature and clinicopathologic features, was constructed and excellently predicted 1-, 2- and 3-year BCR-free survival of localized PCa patients after RP. Gene set enrichment analysis, tumor immunity, and mRNA expression profiling analysis showed that the high-risk group was more prone to the immunosuppressive microenvironment and impaired DNA damage response than the low-risk group. Collectively, we successfully developed a novel 8-gene signature as a powerful predictor for early BCR after RP and created a prognostic nomogram, which may help inform the clinical management of PCa.

Keywords: Prostate cancer, biochemical recurrence, gene signature, risk stratification, biochemical recurrence-free survival

Introduction

Prostate cancer (PCa), the most common site of cancer in aging males, is one of the leading causes of cancer-associated death across the globe. Long-term declines in mortality for PCa have halted, with an estimated 34,130 deaths and 248,530 new cases in 2021 cancer statistics [1]. Biochemical recurrence (BCR) defined by a rise in the blood level of prostate-specific antigen (PSA) is widely used for reporting the outcome of radical prostatectomy (RP). Although PCa has a better overall survival (OS) than other malignancies, its recurrence rate is significantly high with BCR in approximately 20-30% of patients after standard treatment such as RP and radiation therapy [2]. BCR within the first two years after RP is usually consid-

ered to be an early BCR. The patients with BCR, especially with early BCR, are more likely to end up developing clinical recurrence and metastasis, while the median survival for the patients presenting with metastatic PCa is only 30 months [3]. It is thus vital to recognize early BCR in PCa. The serum PSA (sPSA) test has become a routine clinical test for early detection, risk stratification, and monitoring of PCa. But in recent years, sPSA screening test has garnered much criticism for its poor specificity eliciting the potential for overdetection and overtreatment of PCa. In addition, the Gleason score is a decisive prognostic factor recommended by the National Comprehensive Cancer Network (NCCN) Guidelines for PCa, but not perfect due to the limitation of interobserver variability, subjective assessment, and sampling error [4].

With the development of tumor molecular biology, new prediction models based on prognosis-associated genes are emerging and could reflect tumor progression at the molecular level, which might be advantageous to achieve a more accurate prognosis prediction and personalized management of PCa. In fact, with the emergence of gene chips and high-throughput sequencing, it has become a reality that gene signatures derived from abnormal transcriptional profiles can predict prognosis for PCa. In the last decade, multiple gene signatures for PCa prognosis prediction have been proposed. For example, given PCa with heterogeneous hypoxia, Yang *et al.* proposed a 28-gene hypoxia-related signature as a powerful predictor for 5-year BCR-free survival (BFS) in PCa patients after RP or receiving post-prostatectomy radiotherapy independent of clinicopathological factors and commercially available prognostic signatures [5]. Klein *et al.* developed a 17-gene signature, effectively predicting clinical recurrence, PCa-specific death, and adverse pathology [6]. Several other studies also utilized similar methods to construct mRNA expression signatures consisting of various numbers of genes [6-12]. These reports primarily focused on long-term BFS and OS.

Even more successful, three commercialized prognostic gene signatures, Decipher with 22 genes, OncotypeDX Prostate with 17 genes, and Prolaris with 46 genes, are on the market and recommended by the NCCN Guidelines for PCa risk-stratification [13]. Specifically, these three tests can help clinical decision-making for patients with a positive biopsy. Additionally, Decipher and Prolaris are also available for PCa patients undergoing RP to predict tumor progression and thus are helpful in decision-making on secondary treatment. Likewise, only long-term metastasis-free survival data was released for these tests, including 5-year and 10-year metastatic PCa risk. Few studies investigate the molecular signatures for early BCR. In-depth analysis of the public datasets identify prognostic-associated genes and develop a robust gene signature for predicting early BCR, which will help inform clinical management of PCa.

Herein, we constructed an 8-gene signature using the sample data from The Cancer Genome Atlas Project (TCGA) database, following validation in multiple independent cohorts. The predictive performance of our signature for early BCR was compared with that of three commercial panels (Decipher, Oncotype DX, and Prolaris). A nomogram was developed combining this gene signature with independent clinicopathological factors and might provide clinicians with a preferable tool for risk stratification, prognosis prediction, and thus clinical decision-making.

Materials and methods

Data collection

The mRNA expression and clinical data of PCa patients were collected from publicly accessible databases, including TCGA (https://portal.gdc.cancer.gov/), Gene Expression Omnibus (GEO) (https://www.ncbi.nlm.nih.gov/geo/), and German Cancer Research Centre (DKFZ) (https://www.cbioportal.org/study/clinicalData?id=prostate_dkfz_2018). The exploratory TCGA dataset contained 422 PCa samples and 59 normal tissue samples. Two independent GEO datasets with the accessing number of GSE107299 and GSE70769 consisted of 76 and 94 PCa specimens, respectively, and the DKFZ2018 included 292 PCa cases [14].

Differential gene expression analysis

In the TCGA cohort, the raw RNA-Seq count data of the 422 PCa samples and 59 normal tissue samples were normalized, and log2-scale transformed. The differentially expressed genes (DEGs) between PCa and normal sam-

ples were identified using the limma R package [15]. The gene expression data were filtered by count per million >1 in ≥50% of all samples to avoid random correlations between low-expressing genes. The gene was deemed a candidate DEG if a false discovery rate (FDR) of <0.05 and |Log2 fold change| >1 were detected and used for subsequent analysis. A volcano plot of DEGs was drawn using R package ggplot2 (version 3.3.5) and ggrepel (version 0.9.1).

Establishing the 8-gene signature

As previously described [16], a gene signature for BFS prediction was developed. Briefly, we combined the expression level of the screened 1,184 DEGs with the BFS information to establish a multi-gene signature that could predict BFS in PCa. Of note, 60% of the 422-patient TCGA cohort were randomly selected as the training set while the rest 40% as the inner-validation set by adopting the createDataPartition function included in the caret package. DEGs significantly related to BFS were screened out using univariate Cox regression analysis, followed by continuously narrowed-down by LASSO Cox regression analysis designed using the glmnet R package [17]. Then 100 iterations of 10-fold cross-validation with binomial deviance minimization criteria were performed to identify the optimal tuning parameter lambda and corresponding LASSO regression coefficients. The optimal gene set was constructed based lambda according to 1-SE (standard error) rule, and the best combination of genes was determined by best subsets regression using the regsubsets function of the leaps R package [18]. Finally, an 8-gene signature was constructed in the TCGA discovery cohort and presented as a risk score which can be computed for each patient by the following formula:

$$Risk\ Score\ (RS) = \sum_{i}^{n} (Exp * Coefi)$$

Among them, *n* is the number of BFS-associated genes, *Exp* indicates the expression value, and *Coefi* represents the genetic regression coefficient.

Validating the 8-gene signature

The BCR prediction efficiency of the developed 8-gene panel was first confirmed in the inner-validation dataset with 168 patients, which was randomly split from the 422-patient TCGA cohort. The GSE107299, GSE70769, and DKFZ2018 study were served as the separate external validation cohorts. The risk score was computed per the specific risk score formula. The median risk score as a threshold value separated the patients into the high- and low-risk groups. The prognostic differences between the high- and low-risk groups were compared via Kaplan-Meier survival curves combined with a log-rank test. The predictive capability of this signature for 1-, 2-, and 3-year BFS after surgery was assessed by time-dependent receiver operating characteristic (ROC) and concordance index (C-index) analysis. The performance of this gene signature was also detected in the subgroup of the discovery cohort and compared with that of three commercial prognostic gene panels.

Identifying the independent predictors for BCR

To identify independent markers of BCR in PCa, the 8-gene signature and other clinical parameters, including age, Gleason score, clinical TNM stage, pathologic TNM stage, sPSA, and lymph node involvement (LNI), were submitted to Cox regression analyses.

Developing a predictive nomogram

All significant prognostic markers selected by Cox regression analysis were combined to construct a nomogram using cph function from the rms package, allowing for predicting 1-, 2-, and 3-year BFS of PCa patients in the TCGA dataset. The nomogram's discrimination, calibration, and reliability were assessed, wherein the discrimination was evaluated by C-index, the calibration by comparing predicted and observed OS, and the reliability via decision curve analysis (DCA).

Restricted mean survival time (RMST) analysis

In longitudinal clinical studies to compare two groups, RMST is useful in quantifying underlying differences concerning a time-to-event endpoint. RMST analysis was used in the discovery cohort to examine BFS rates in the high- and low-risk groups at different time points (5 and 10 years of follow-up) via the 'survRM2' package.

Gene set enrichment analysis

Gene set enrichment analysis (GSEA) was conducted in the TCGA cohort to identify gene sets whose expression was enriched or depleted in the high- and low-risk patients using the GSEA function of clusterProfiler R package. The enriched or depleted gene sets correlated with survival were identified via Molecular Signatures Database v.7.4 [19].

Tumor immunity and mRNA expression profiling analysis

xCell, a novel method integrating the advantages of gene set enrichment with deconvolution algorithm, can estimate the scores of 64 infiltrating cell subtypes using the normalized RNA-seq data [20]. Here, the xCell algorithm was adopted to characterize the tumor microenvironment (TME) of PCa tissues in the high- and low-risk groups and further investigated the association between the risk score and the immune infiltrate in the TCGA discovery cohort.

The mRNA expression of genes associated with TME and DNA damage response in PCa was also analyzed in the two risk groups. The expression of TME and DNA damage response-related genes was visualized using ggboxplot function in R package ggpubr (version 0.4.0), and was compared by Student *t* test between the high- and low-risk groups. Heat maps were plotted using R package pheatmap (version 1.0.12). P-values for high-risk versus low-risk groups were added using the function stat_compare_means in the boxplots.

Statistical analyses

All analytical methods above and R packages were conducted by R software v 4.0 (R Foundation for Statistical Computing, Vienna, Austria). Cox and LASSO regression were utilized to screen the BFS-related variables. The log-rank test was adopted to compare Kaplan-Meier curves. Unless otherwise stipulated, a *P*-value below 0.05 was considered statistically significant.

Results

Identifying DEGs

A flowchart was graphed to describe this study visually (**Figure 1A**). Through analysis of gene expression data of 422 primary PCa samples and 59 normal tissue samples in the TCGA discovery cohort, a total of 1,184 DEGs were identified, consisting of 333 up-regulated and 851 down-regulated genes in tumor tissues (**Figure 1B**). DLX1 showed the most significant differential expression, up-regulated approximately 55-fold in tumor tissue (**Figure 1B**).

Screening BFS-correlated DEGs and establishing the 8-gene prognostic signature

The 422-patient TCGA cohort was randomly assigned in a 6:4 ratio into a training dataset (N=254) and an inner-validation dataset (N=168). The DEGs with significant prognostic values were first screened out in the training dataset via univariate Cox proportional hazards regression analysis and then were narrowed down by a LASSO Cox regression model and an all subset regression model. Finally, eight genes associated with PCa prognosis, including spectrin beta non-erythrocytic 2 gene (*SPTBN2*), leucine-rich glioma inactivated 3 (*LGI3*), Transglutaminase 3 (*TGM3*), leukocyte receptor cluster member 9 (*LENG9*), hyaluronan synthase 3 (HAS3), uncoupling protein-4 (UCP4/SLC25A27), protocadherin gamma-A1 (PCDHGA1), and ADP-Ribosylhydrolase Like 1 (ADPRHL1) were identified using the regsubsets function of the leaps R package and then used to establish the prognostic gene signature. The down-regulated *HAS3*, *LENG9*, *ADPRHL1*, and *TGM3* were deemed tumor suppressors, and the up-regulated *PCDHGA1*, *LGI3*, *SPTBN2*, and *SLC25A27* were considered as oncogenes (**Figure 1C**). Then the risk score for prognosis prediction was computed according to following formula: risk score = $(1.029\times Exp_{SPTBN2}) + (0.851\times Exp_{LGI3}) + (-0.273\times Exp_{TGM3}) + (-0.613\times Exp_{LENG9}) + (-0.866\times Exp_{HAS3}) + (1.203\times Exp_{SLC25A27}) + (0.204\times Exp_{PCDHGA1}) + (-0.342\times Exp_{ADPRHL1})$.

Validating the 8-gene signature

The median risk score of 0.79 was determined as the optimal threshold for risk stratification of PCa patients in the training dataset, while this cut-off value of 0.79 also served as a risk indicator for both the inner-validation dataset and the whole TCGA dataset. After stratification, the high-risk group separately comprised 127 patients in the training dataset, 92 in the inner-validation dataset, and 219 in the entire TCGA

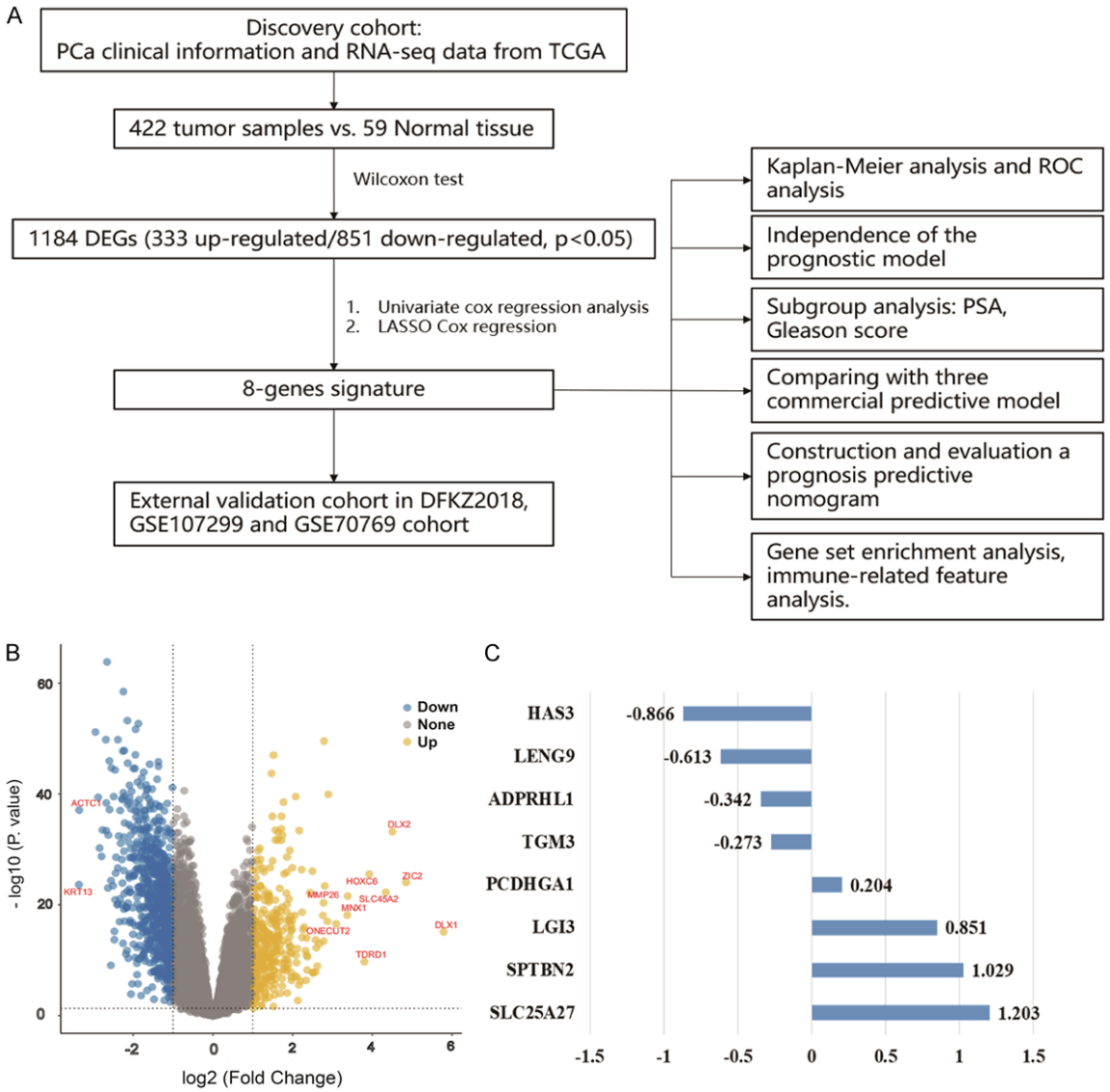

Figure 1. Screening BFS-correlated DEGs and establishing the 8-gene prognostic signature. A. The flow chart presents the process of establishing the gene signature and prognostic nomogram for PCa. B. The volcano plot displays the DEGs, which meet the criteria of a false discovery rate of <0.05, and |log2 fold change| >1. C. Eight BFS-correlated DEGs are shown with corresponding estimated regression coefficients. BFS: biochemical recurrence-free survival; DEGs: differentially expressed genes; PCa: prostate cancer.

dataset. The clinicopathological features in the high- and low-risk patients of the TCGA dataset were compared using the twogrps function in R package CBCgrps (version 2.8.2), wherein no significant differences were seen among all the clinical characteristics between the two groups (**Table 1**). Time-dependent ROC and Kaplan-Meier curves were utilized to assess the performance of this 8-gene signature for the prediction of 1-, 2-, and 3-year BFS. As shown in the top panels of **Figure 2A-C**, the area under the ROC curve (AUC) values for 1-, 2-, and 3-year BFS predictions were 0.705, 0.732, and 0.751 for the training dataset, 0.822, 0.791, and 0.707 for the inner-validation dataset, and 0.737, 0.760, and 0.737 for the entire TCGA cohort, respectively. Kaplan-Meier plots indicated that in all three datasets, a significantly poor BFS existed in the patients with high-risk scores compared to the patients with low-risk scores (P=0.003 for the training dataset, P=0.0069 for the inner-validation dataset, and P<0.0001 for the entire TCGA discovery cohort) (**Figure 2A-C**, bottom panels). The

Table 1. Comparison of clinical baseline characteristics between the high- and low-risk patients in the TCGA cohort

Variables	Total (n=422)	High-risk (n=219)	Low-risk (n=203)	*p* value
Age, Median (Q1, Q3)	61 (56, 66)	61 (56, 65.5)	62 (57, 66)	0.12
gleason_score, n (%)				0.804
≤6	39 (9)	19 (9)	20 (10)	
>6	383 (91)	200 (91)	183 (90)	
clinical_T, n (%)				0.661
T1/2	304 (86)	157 (85)	147 (88)	
T3/4	48 (14)	27 (15)	21 (12)	
clinical_M, n (%)				1
M0	397 (99)	202 (100)	195 (99)	
M1	2 (1)	1 (0)	1 (1)	
pathologic_T, n (%)				0.402
pT1/2	153 (37)	75 (35)	78 (39)	
pT3/4	264 (63)	142 (65)	122 (61)	
pathologic_N, n (%)				0.154
N0	302 (82)	151 (79)	151 (85)	
N1	66 (18)	40 (21)	26 (15)	
psa_value, n (%)				0.642
<10	396 (97)	202 (96)	194 (97)	
≥10	13 (3)	8 (4)	5 (3)	
LNI, n (%)				1
No	60 (14)	31 (14)	29 (14)	
Yes	362 (86)	188 (86)	174 (86)	
radiation_therapy, n (%)	31 (7)	14 (6)	17 (8)	0.586
No	337 (80)	179 (82)	158 (78)	
Yes	54 (13)	26 (12)	28 (14)	
residual_tumor, n (%)	10 (2)	4 (2)	6 (3)	0.437
R0	269 (64)	139 (63)	130 (64)	
R1	128 (30)	69 (32)	59 (29)	
R2	3 (1)	0 (0)	3 (1)	
RX	12 (3)	7 (3)	5 (2)	

RMST for the whole TCGA cohort was also evaluated. The 5- and 10-year RMST were 4.16 (95% CI, 3.92-4.40) and 6.99 (95% CI, 6.07-7.91) years for the high-risk group, and 4.70 (95% CI, 4.55-4.84) and 8.98 (95% CI, 8.50-9.50) years for the low-risk group with significant difference between the high- and low-risk groups in 5- (P=0.0003) and 10-year (P=0.0005) (**Figure 2D**). Subgroup analysis showed that when patients were stratified by PSA level, the patients with a PSA level of ≤10 or 20 ng/ml had a significantly favorable prognosis versus the patients with a PSA level of >10 or 20 ng/ml, while 8-gene signature-based risk group stratification still performed well in predicting BFS in the subgroup with a PSA level of ≤10 or 20 ng/ml (**Figure 2E** and **2F**). Similarly, 8-gene signature-based risk group stratification also performed well in the subgroup with clinically staged T1-2, M0, or pathologically staged N0 PCa (Supplementary Figure 1). These results indicated that the 8-gene signature was an effective predictor of BFS for PCa patients even across subgroups stratified according to PSA level or TNM status.

To confirm the predictive value of this signature, three external sets, DKFZ2018, GSE107299, and GSE70769, were utilized to assess the findings from the discovery cohort. The AUC values for predicting 1-, 2-, and 3-year BFS were 0.803, 0.793, and 0.834 for the

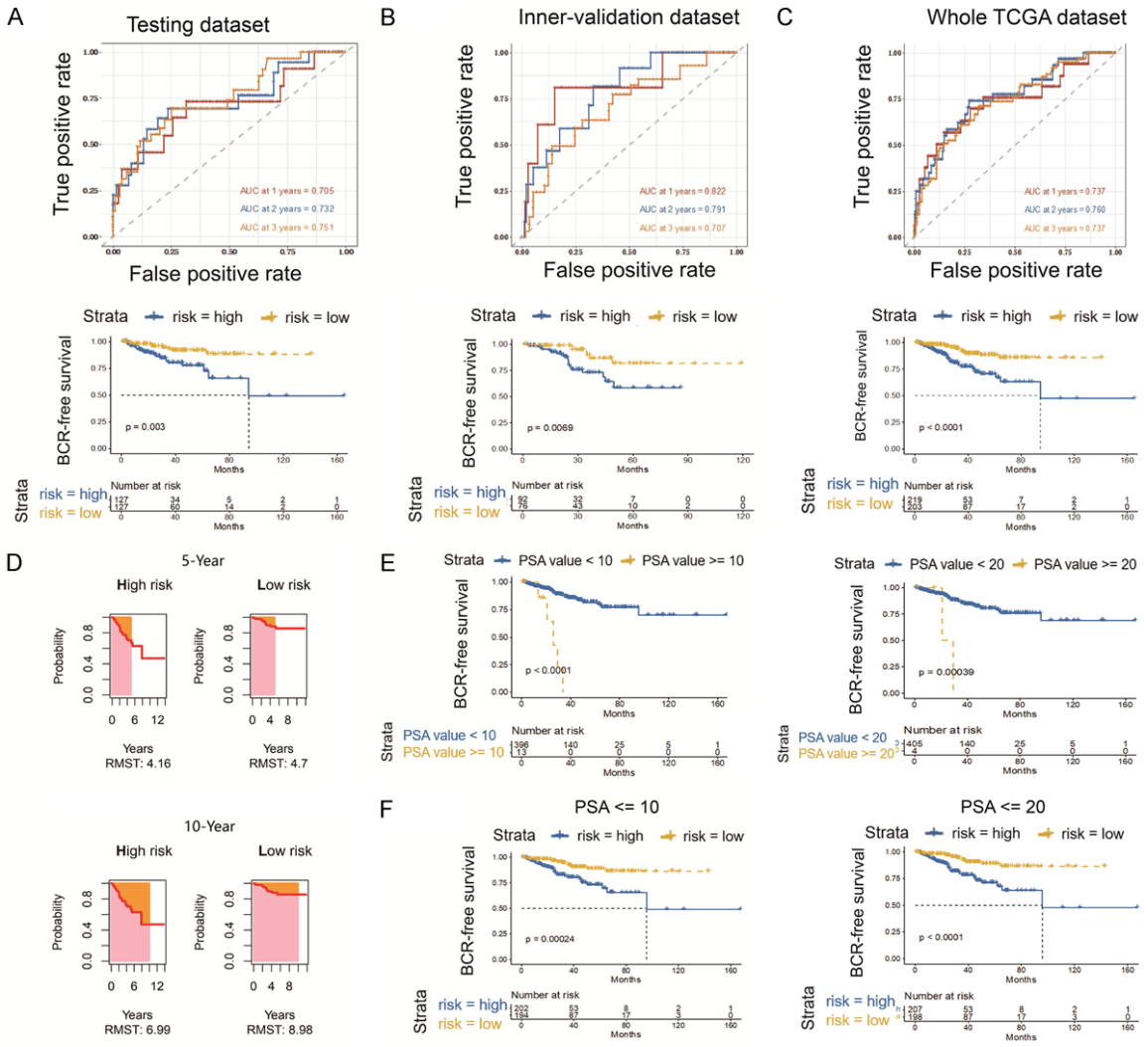

Figure 2. Prognostic analysis and performance evaluation of the 8-gene signature in the discovery set. The time-dependent ROC analyses and Kaplan-Meier analysis of the 8-gene signature for predicting 1-, 2-, and 3-year BFS in the training dataset (A), inner-validation dataset (B), and whole TCGA dataset (C). Patients are stratified into high- and low-risk groups with a cut-off of the median value in the training set. (D) The 5- and 10-year RMST of the high- and low-risk groups in the TCGA discovery cohort. (E) Kaplan-Meier curves for BFS in the patients with low and high PSA levels (cut-off value 10 or 20 ng/ml). (F) Kaplan-Meier BFS analyses of the 8-gene predicative model in the subgroup with a PSA level of ≤10 or 20 ng/ml. ROC: receiver operating characteristic; BFS: biochemical recurrence-free survival; RMST: restricted mean survival time; TCGA: The Cancer Genome Atlas Project; PSA: prostate-specific antigen.

DKFZ2018 dataset, 0.759, 0.743, and 0.727 for the GSE107299 dataset, and 0.646, 0.770, and 0.733 for the GSE70769 dataset, respectively (**Figure 3A-C**, top panels). Patients were classified into the high- and low-risk groups using the median risk score derived from each dataset. As expected, the high-risk group had a significantly inferior BFS as compared to the low-risk group (P=0.019 for the DKFZ2018 dataset, P<0.0001 for the GSE107299 dataset, and P=0.0015 for the GSE70769 dataset) (**Figure 3A-C**, bottom panels).

Comparing the 8-gene signature with commercial prognostic gene panels

In addition, in view that the marketed Decipher, Oncotype DX Prostate, or Prolaris tumor-based molecular panel has been recommended by the NCCN Guidelines for initial risk stratification in the appropriate PCa patients, the performance of this 8-gene signature was also evaluated via comparison with that of these three commercial prognostic gene products. The genes of these three commercial panels were

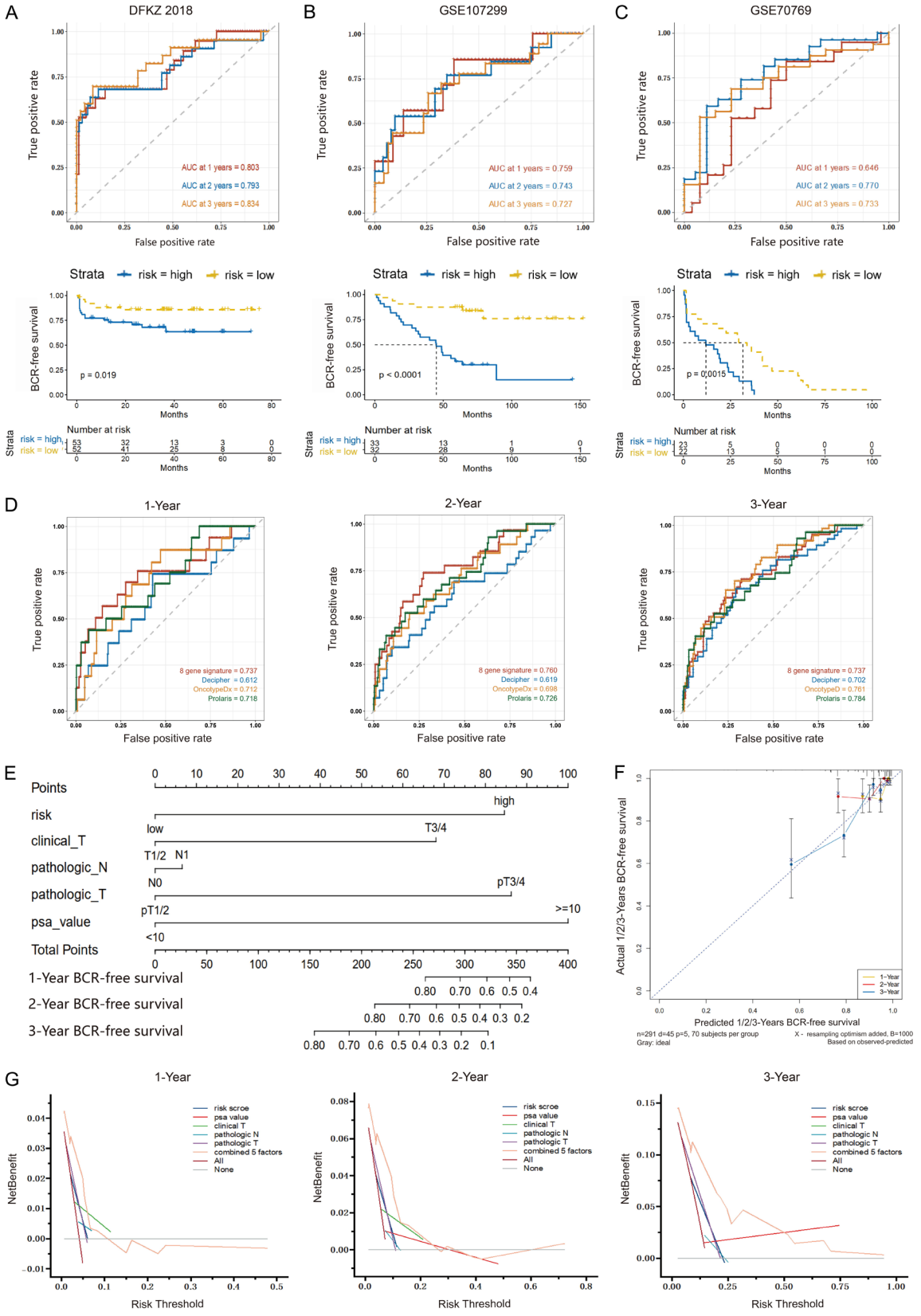

Figure 3. Validation of the 8-gene signature. The time-dependent ROC and Kaplan-Meier curves for evaluating the performance of the 8-gene signature in the validation datasets, DFKZ 2018 (A), GSE107299 (B), and GSE70769 (C). (D) Comparison of the 8-gene signature with three commercial panels using ROC analyses for predicting 1-,

2- and 3-year BFS. (E) The nomogram plot for predicting 1-, 2- and 3-year BFS in PCa patients. (F) The calibration curves of the nomogram showing the probability of BFS at 1-, 2- and 3-year after radical prostatectomy. (G) The DCA curves comparing the net clinical benefit among all significant clinical factors, including the nomogram. ROC: receiver operating characteristic; BFS: biochemical recurrence-free survival; DCA: decision curve analysis.

Table 2. Univariate and multivariate Cox regression analyses of risk score and clinical pathological variables in the TCGA cohort

Characteristics	No Of Pts	Univariate Cox		Multivariate Cox	
		HR (95% CI)	*P*. value	HR (95% CI)	*P*. value
Age (≥60 vs. <60)	422	1.52 (0.88-2.65)	0.1300		
Gleason score (>6 vs. ≤6)	422	2.71 (0.66-11.12)	0.1500		
Clinical M (M1 vs. M0)	399	0 (0-Inf)	0.8200		
Clinical T (T3/4 vs. T1/2)	352	3.9 (2.16-7.04)	1.00E-06	2.57 (1.33-4.94)	0.0047
Pathologic N (N1 vs. N0)	368	1.84 (1-3.4)	0.0470	1.1 (0.55-2.17)	0.7900
Pathologic T (pT3/4 vs. pT1/2)	417	5.4 (2.31-12.6)	1.20E-05	3.31 (1.24-8.84)	0.0170
PSA (≥10 vs. <10)	409	9.14 (3.57-23.43)	2.10E-08	4 (1.37-11.68)	0.0110
LNI (Yes vs. No)	417	2.04 (0.74-5.63)	0.1600		
LNI_N (≥ median vs. < median)	366	0.6 (0.34-1.06)	0.0740		
Risk (High vs. Low)	422	0.32 (0.18-0.57)	5.30E-05	0.31 (0.15-0.62)	0.00094

listed in Supplementary Table 1. As demonstrated by time-dependent ROC curves in **Figure 3D** and Supplementary Table 2, the AUC values of the 8-gene signature were numerically higher than those of three commercial panels for predicting 1- and 2-year BFS (1-year AUC: 0.737 vs. 0.612, 0.712, and 0.718; and 2-year AUC: 0.760 vs. 0.619, 0.698, and 0.726), though the differences were not significant. For 3-year BFS prediction, the AUC values of the 8-gene signature and three commercial panels were similar (3-year AUC: 0.737 vs. 0.702, 0.761, and 0.784). Additionally, the C-index of this signature was also comparable to that of three commercial panels (0.646 vs. 0.639, 0.669, and 0.650). These results revealed the 8-gene signature's good performance for early BCR prediction in PCa.

Identifying the independent prognostic markers and building a predictive nomogram

The independent prognostic factors for PCa were determined by Cox regression analyses of data from the TCGA cohort. The unadjusted univariate Cox regression analysis revealed that clinical T stage (P<0.001), pathologic N (P=0.047), and T stage (P<0.001), PSA (P< 0.001), and 8-gene signature-based risk group classifier (P<0.001) were significantly correlated with BFS in PCa patients. In addition, multivariate Cox regression analysis displayed that risk score remained a strong predictor for BFS alongside clinical T stage, pathologic T stage, and PSA (**Table 2**).

For the development of a more reliable prediction tool for clinical practice, a nomogram was established via integrating all significant clinical factors, including the risk score, clinical T stage, pathologic N and T stage, and PSA, to predict 1-, 2- and 3-year BFS in PCa (**Figure 3E**). Calibration plots showed the nomogram with a strong predictive ability for 1-, 2-, and 3-year BFS, as demonstrated by the consistency between predicted and actual survival time (**Figure 3F**). DCA curves showed that the net clinical benefit of the nomogram was higher than that of any other character alone (**Figure 3G**). Additionally, the C-index of 0.742 for the nomogram was the highest among all factors determined.

Gene set enrichment analyses

GSEA analysis was implemented between the high-/low-risk score tumor samples and normal tissues in the TCGA cohort to investigate the underlying molecular mechanism of the 8-gene signature. **Figure 4A** and **4B** showed the hallmarks with significant differences, and the top 5 hallmarks were listed in **Table 3**. Compared with normal tissues, the tumor samples from the two risk groups showed the up-regulation of "MYC targets V1" and the suppression of "epithelial-mesenchymal transition". In addition, hallmarks "myogenesis", "apoptosis", and

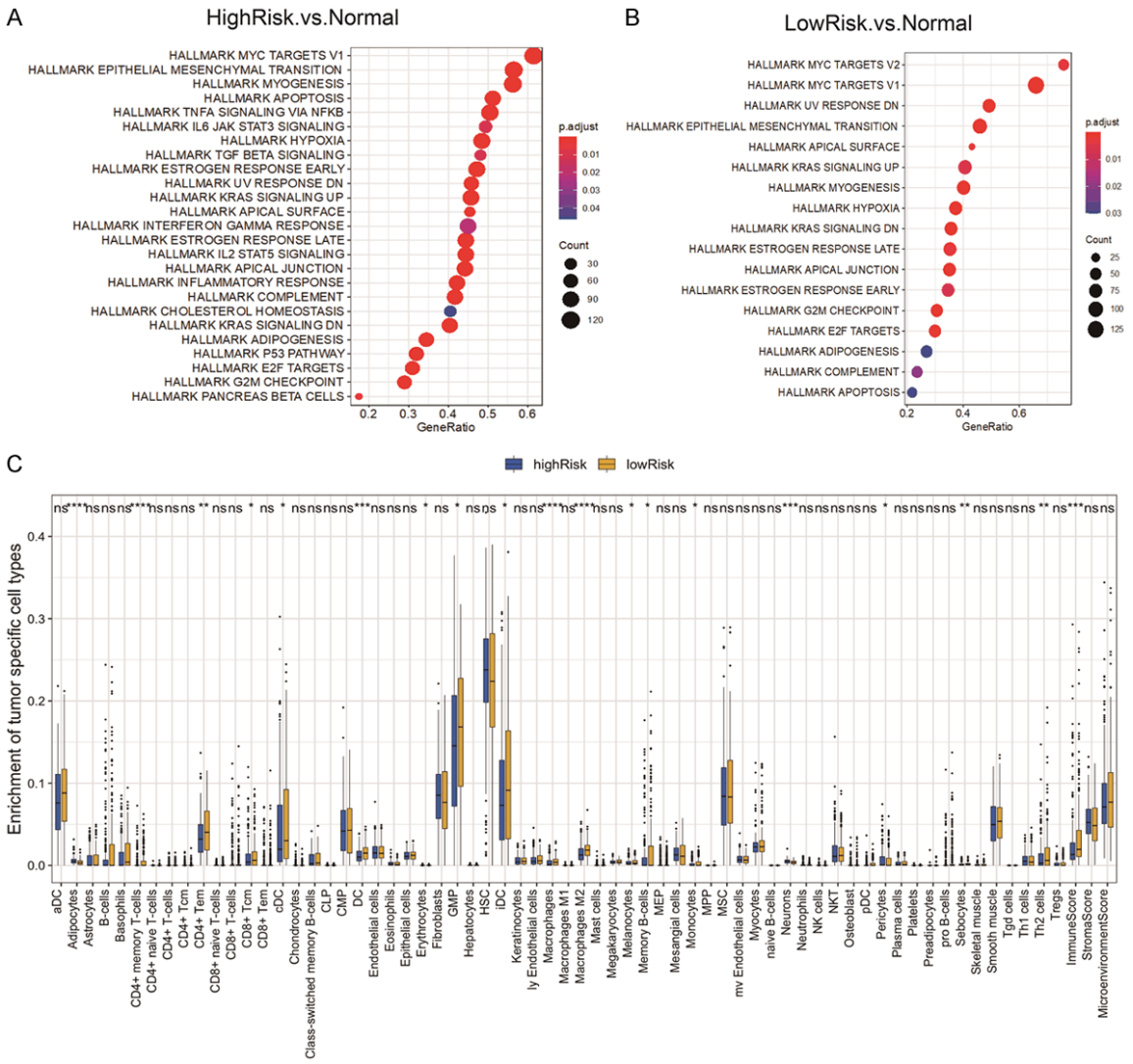

Figure 4. Gene set enrichment analyses, tumor immunity, and mRNA expression profiling analysis. A, B. Gene set enrichment analyses are conducted between the high-/low-risk tumor samples and normal tissues in the TCGA discovery cohort to identify enriched or depleted gene sets. C. Difference analysis of 64 immune cells infiltration between the high- and low-risk groups in the TCGA cohort using xCell algorithm. *P<0.05, **P<0.01, ***P<0.001, and ****P<0.0001.

"TNF-α signaling via NF-κB" were also inhibited in the high-risk group, whereas "MYC targets V2" was highly expressed and "UV response DN" and "apical surface" were inhibited in the low-risk group compared to normal tissues (**Table 3**). These results revealed different biological features between the high- and low-risk groups.

Correlation with the infiltration levels of immune cells

Through the xCell algorithm, we investigated the relationship between this 8-gene signature and the immune infiltrate. Among the 64 subtypes of immune cells in tumors determined via xCell, the low-risk group was more infiltrated by multiple subtypes of immune cells, including memory B cells, T helper 2 cells, central memory CD8 T cells, CD4+ memory T cells, CD4+ naive T cells, activated dendritic cells, monocytes, as well as M2-polarized macrophages than the high-risk group (**Figure 4C**). Besides, the immune score is higher in the low-risk group than in the high-risk group (**Figure 4C**).

mRNA expression analysis

In view that the immunotherapeutic benefits were associated with immune checkpoint high

Table 3. Significantly enriched hallmarks in the TCGA cohort by GSEA

NAME	SIZE	NES	NOM p-val	FDR q-val	Groups
HALLMARK_MYC_TARGETS_V1	200	1.699985701	0.000137665	6.09E-05	HighRisk vs. Normal
HALLMARK_EPITHELIAL_MESENCHYMAL_TRANSITION	200	-2.167283953	1.67E-09	7.37E-10	HighRisk vs. Normal
HALLMARK_MYOGENESIS	199	-2.766214294	1.67E-09	7.37E-10	HighRisk vs. Normal
HALLMARK_APOPTOSIS	160	-1.910151921	1.10E-05	4.86E-06	HighRisk vs. Normal
HALLMARK_TNFA_SIGNALING_VIA_NFKB	200	-2.209713985	1.67E-09	7.37E-10	HighRisk vs. Normal
HALLMARK_MYC_TARGETS_V2	58	1.748083455	0.004336176	0.002738637	LowRisk vs. Normal
HALLMARK_MYC_TARGETS_V1	200	1.936585623	2.67E-07	1.69E-07	LowRisk vs. Normal
HALLMARK_UV_RESPONSE_DN	144	-1.873905197	0.000107974	6.82E-05	LowRisk vs. Normal
HALLMARK_EPITHELIAL_MESENCHYMAL_TRANSITION	200	-1.808381186	0.000177091	0.000111847	LowRisk vs. Normal
HALLMARK_APICAL_SURFACE	44	-1.875651113	0.003511655	0.002217887	LowRisk vs. Normal

expression, IFNγ pathway activation, T cell activation, and activated tumor microenvironment, we also evaluated the mRNA expression of common immune checkpoints, and representative genes of IFNγ pathway, effector T cell, T cell receptor, and the tumor microenvironment in the high- and low-risk patients of the TCGA dataset (Supplementary Figure 2A-D). In the tested immune checkpoints (*PD-1*, *PD-L1*, *PD-L2*, *LAG3*, *CTLA-4*, *TIM3*, and *VTCN1*), only the mRNA expression of *PD-L1* and *TIM3* was nearly significantly (P=0.0655) or significantly (P=0.0097) different between the two groups, both lower in the high-risk group than in the low-risk group. In terms of the activity of the IFNγ pathway, T cell, and TME, the high-risk group had significantly lower mRNA expression in some representing genes than the low-risk group, including *GZMB*, *IFI16*, *IFI30*, *IRF1*, *CD3D*, *CD4*, *CD74*, *GRAP2*, *IL2RB*, *IL1B*, *IL6*, *PTGS2*, and *TNF*, suggesting that high-risk score was associated with the immunosuppressive microenvironment (Supplementary Figure 3A-D). Additionally, the mRNA expression of DNA damage repair (DDR) genes was also analyzed. Among 106 DDR genes analyzed, the high-risk group had 11 up-regulated and 31 down-regulated genes compared with the low-risk group (Supplementary Figures 2E, 3E; Supplementary Table 3). These findings suggested that high-risk patients are more likely to have immunosuppressive microenvironment and DNA damage response than low-risk patients.

Discussion

PCa is one of the most deadly urinary tumors in males globally. Progression to BCR is a significant turning point in PCa development. Once BCR, the majority of PCa patients will metastasize, leading to ultimate death [21]. Early BCR accounts for nearly half of all tumor BCR following RP, and PCa patients with early BCR always suffer from dismal long-term outcomes compared with those without early BCR, although significant progress has been made in adjuvant therapy. Therefore, it is advisable to effectively stratify PCa with a high risk of early BCR after RP, so as to carry out early intervention before the progression of metastasis.

Herein, an 8-gene signature for predicting early BCR was established using gene expression and BFS data from the TCGA PCa cohort. In the light of the risk scores computed based on the expression level of 8 genes, patients in the discovery dataset can be separated into the high- and low-risk groups with significant differences in BFS and 5- and 10-year RMST. This gene classifier also effectively helped stratify patients with a PSA level of ≤10 or 20 ng/ml into different risk groups. Besides, it was successfully validated in three external datasets that this gene panel significantly discriminated between the high- and low-risk groups for BFS. This 8-gene classifier was also an independent predictor of BFS. A nomogram was developed via integrating the 8-gene classifier and clinicopathological indicators, which could precisely predict BFS. Additionally, it was noteworthy that the high-risk patients were more prone to the immunosuppressive microenvironment and DDR variations than the low-risk patients.

Among the eight genes included in this panel, six of them have been experimentally verified to be associated with cancer. HAS3, one family member of HSA, is responsible for producing both secreted and cell-associated forms of hyaluronan and has been widely reported to be linked to tumor progression, metastasis, and

poor prognosis in multiple human cancers. It has been documented that the increase of HAS3 expression is associated with a dismal prognosis in oral cancer and breast cancer [22, 23]. Up-regulation of HAS3 could enhance the proliferation of gastric cells and colon cancer cells [24, 25]. Consistently, HAS3 down-regulation is also reported to be an indicator of poor outcome in urothelial carcinoma of the upper urinary tract and the bladder [26]. The anticancer effect of HAS3 remains controversial. Consistently, in PCa, HAS3 has been demonstrated to promote the growth of TSU PCa cells but inhibit the cell proliferation and migration of LNCap PCa cells [27, 28]. ADPRHL1 is a pseudoenzyme expressed in the developing heart myocardium of all vertebrates. Wan et al. reported that ADPRHL1 might play a critical role in the recurrence of uveal melanoma [29]. But the role of ADPRHL1 in PCa is not revealed. TGM3, one of the critical enzymes contributing to the formation of protein polymers in the epidermis and the hair follicle, has been reported as a tumor suppressor involved in the modulation of cell proliferation, epithelial-to-mesenchymal transition, apoptosis in colorectal cancer, esophageal cancer, and hepatocellular carcinogenesis [30-33]. However, the association of TGM3 with PCa has not ever been reported. LGI3, a secreted protein that belongs to LGI/epitempin family, is highly expressed in the brain and regulates neuronal exocytosis and differentiation [34, 35]. In the last few years, some studies documented that the high expression of LGI3 is associated with favorable outcomes in glioma and non-small cell lung cancer, which might be attributed to increased innate tumor immunity in the tumor microenvironment [36, 37]. Hence, LGI3 might be a potential therapeutic target in PCa. SPTBN2 belonging to the spectrin family is widely reported to act as a structural carrier for stabilizing and activating membrane channels, receptors, and transporters involved in neurogenesis and degenerative diseases. Increasing evidence points out that SPTBN2 could serve as a crucial clinical parameter of tumor progression and survival for some cancers, such as ovarian cancer, bladder cancer, and colorectal cancer patients with m6A modifications [38, 39]. Moreover, Wen *et al.* identified SPTBN2 as a signature gene, emerging in pathogenesis and pattern recognition of seven common cancers [40]. However, the exact role of SPTBN2 in PCa is still unknown. SLC25A27 encodes a neuronal mitochondrial uncoupling protein-4 (UCP4), which protects neurons against oxidative stress and mitochondrial dysfunction [41, 42]. It has been discovered that the positivity of UCP4 is associated with classical prognostic factors such as lymph node metastases, p53 and Ki-67 in breast carcinomas. As yet it is not clear whether UCP4 is related to PCa. PCDHGA1, a member of the protocadherin family, mediates the formation and maintenance of specific synaptic connections [43]. LENG9 is a member of the leukocyte receptor complex [44]. They have never been documented associated with cancer to date. Further investigation of the role of above-mentioned genes in PCa are in our plan.

In comparison with several existing gene signatures, our multi-gene panel demonstrated sound performance in risk stratification of BCR, wherein its AUCs for 1-, 2-, and 3-year BFS in the discovery cohort were 0.737, 0.760, and 0.737, respectively, and remained stable in three external validation sets. For example, Yuan *et al*. developed a 4-gene signature, and its AUCs for 1- and 3-year BFS in the training set are 0.83 and 0.799, respectively, but its AUCs in the validation set are 0.638 and 0.723, respectively [7]. Long *et al*. also developed a 4-gene signature, and its AUCs for 1-, 2- and 3-year BFS are 0.827, 0.774 and 0.810 for the training set, and 0.718, 0.675, and 0.638 for the validation set [45]. Lv et al. established a 5-immune-related gene signature, and its AUC for 3-year BFS is 0.71 for the training dataset and 0.775 for the validation dataset [46]. In addition, our multi-gene panel had superior performance in predicting early BCR compared with three commercial panels in terms of AUC values for 1- and 2-year BFS prediction and C-index. Early BCR risk stratification tools have significant clinical value in personalized therapy. The patients with low-risk early BCR could be managed by active surveillance, while those with high-risk early BCR may require adjuvant therapies or/and closer clinical management. Given that this signature could be used for risk stratification in the subgroup with a PSA level of ≤10 or 20 ng/ml or a low TNM-stage, our signature may help identify low-risk patients more accurately, avoid unnecessary overtreatment, and select an optimal management strategy.

In addition, this signature might reflect the changes of TME from different aspects as shown by xCell and mRNA expression profiling, which offered convenience to monitor the infiltration of immune cells and the potentiality to assist rational diagnosis and individualized treatment. DNA damage is a primary driver of cancer initiation and progression, while loss-of-function alterations of DDR genes promote a more aggressive PCa phenotype [47, 48]. A recent study has shown that the DDR alteration signature has a substantial prognostic value and may be utilized for risk stratification in PCa [45]. More instructively, DDR could help guide clinical decision-making in PCa. For example, DDR deficiency has been well-documented as a predictor of sensitivity to platinum agents in castration-resistant PCa [49-51]; and the FDA has approved olaparib for use in metastatic castration-resistant PCa patients with a pathogenic mutation in a homologous recombination repair gene and previous experience of enzalutamide or abiraterone therapy [52]. We consistently found that the high-risk score patients had a more severe DNA damage response than the low-risk score patients, which might provide treatment information for the patients with future relapse.

Some limitations still exist in this study. Firstly, this study is performed based on available retrospective data derived from public datasets, and thus it should be regarded as indicative for future research rather than conclusive. Secondly, most patients in these datasets were the European American population. Therefore extrapolating these results to the patients of other ethnicities should be done with caution. Thirdly, the underlying molecular mechanisms of the selected eight genes in early BCR of PCa remain to be further explored. To summarize, our study built an 8-gene signature that can reliably predict early BCR after RP, which will contribute to the personalized management of PCa patients.

Acknowledgements

We thank the patients and investigators who participated in TCGA, GEO and German Cancer Research Centre for providing data.

Disclosure of conflict of interest

None.

Address correspondence to: Qi Shen, The Second Clinical Medical College of Jinan University, Shenzhen People's Hospital, The First Affiliated Hospital of South University of Science and Technology of China, No. 1017 Dongmen North Road, Luohu District, Shenzhen 518000, China. E-mail: 25nancy@163.com; Wei Wei, Department of Urology, Hwa Mei Hospital, University of Chinese Academy of Sciences, Northwest Street 41, Haishu District, Ningbo 315000, Zhejiang, China. E-mail: weiwei_nb@163.com

References

[1] Siegel RL, Miller KD, Fuchs HE and Jemal A. Cancer statistics, 2021. CA Cancer J Clin 2021; 71: 7-33.

[2] Shao N, Wang Y, Jiang WY, Qiao D, Zhang SG, Wu Y, Zhang XX, Wang JL, Ding Y and Feng NH. Immunotherapy and endothelin receptor antagonists for treatment of castration-resistant prostate cancer. Int J Cancer 2013; 133: 1743-1750.

[3] Kessler B and Albertsen P. The natural history of prostate cancer. Urol Clin North Am 2003; 30: 219-226.

[4] Randall EC, Zadra G, Chetta P, Lopez BG, Syamala S, Basu SS, Agar JN, Loda M, Tempany CM and Fennessy FM. Molecular characterization of prostate cancer with associated Gleason score using mass spectrometry imaging. Mol Cancer Res 2019; 17: 1155-1165.

[5] Yang L, Roberts D, Takhar M, Erho N, Bibby BAS, Thiruthaneeswaran N, Bhandari V, Cheng WC, Haider S, McCorry AMB, McArt D, Jain S, Alshalalfa M, Ross A, Schaffer E, Den RB, Jeffrey Karnes R, Klein E, Hoskin PJ, Freedland SJ, Lamb AD, Neal DE, Buffa FM, Bristow RG, Boutros PC, Davicioni E, Choudhury A and West CML. Development and validation of a 28-gene hypoxia-related prognostic signature for localized prostate cancer. EBioMedicine 2018; 31: 182-189.

[6] Klein EA, Cooperberg MR, Magi-Galluzzi C, Simko JP, Falzarano SM, Maddala T, Chan JM, Li J, Cowan JE, Tsiatis AC, Cherbavaz DB, Pelham RJ, Tenggara-Hunter I, Baehner FL, Knezevic D, Febbo PG, Shak S, Kattan MW, Lee M and Carroll PR. A 17-gene assay to predict prostate cancer aggressiveness in the context of Gleason grade heterogeneity, tumor multifocality, and biopsy undersampling. Eur Urol 2014; 66: 550-560.

[7] Yuan P, Ling L, Fan Q, Gao X, Sun T, Miao J, Yuan X, Liu J and Liu B. A four-gene signature associated with clinical features can better predict prognosis in prostate cancer. Cancer Med 2020; 9: 8202-8215.

[8] Chen X, Xu S, McClelland M, Rahmatpanah F, Sawyers A, Jia Z and Mercola D. An accurate prostate cancer prognosticator using a seven-gene signature plus Gleason score and taking cell type heterogeneity into account. PLoS One 2012; 7: e45178.
[9] Jiang Y, Mei W, Gu Y, Lin X, He L, Zeng H, Wei F, Wan X, Yang H, Major P and Tang D. Construction of a set of novel and robust gene expression signatures predicting prostate cancer recurrence. Mol Oncol 2018; 12: 1559-1578.
[10] Hu D, Jiang L, Luo S, Zhao X, Hu H, Zhao G and Tang W. Development of an autophagy-related gene expression signature for prognosis prediction in prostate cancer patients. J Transl Med 2020; 18: 160.
[11] Liu B, Li X, Li J, Jin H, Jia H and Ge X. Construction and validation of a robust cancer stem cell-associated gene set-based signature to predict early biochemical recurrence in prostate cancer. Dis Markers 2020; 2020: 8860788.
[12] Shao N, Tang H, Mi Y, Zhu Y, Wan F and Ye D. A novel gene signature to predict immune infiltration and outcome in patients with prostate cancer. Oncoimmunology 2020; 9: 1762473.
[13] (NCCN) NCCN. NCCN Clinical practice guidelines in oncology. Prostate Cancer. Version 2. 2021. 2021.
[14] Gerhauser C, Favero F, Risch T, Simon R, Feuerbach L, Assenov Y, Heckmann D, Sidiropoulos N, Waszak SM and Hübschmann D. Molecular evolution of early-onset prostate cancer identifies molecular risk markers and clinical trajectories. Cancer Cell 2018; 34: 996-1011.
[15] Ritchie ME, Phipson B, Wu D, Hu Y, Law CW, Shi W and Smyth GK. Limma powers differential expression analyses for RNA-sequencing and microarray studies. Nucleic Acids Res 2015; 43: e47.
[16] Zhou T, Cai Z, Ma N, Xie W, Gao C, Huang M, Bai Y, Ni Y and Tang Y. A novel ten-gene signature predicting prognosis in hepatocellular carcinoma. Front Cell Dev Biol 2020; 8: 629.
[17] Friedman J, Hastie T and Tibshirani R. Regularization paths for generalized linear models via coordinate descent. J Stat Softw 2010; 33: 1.
[18] Farkas O and Héberger K. Comparison of ridge regression, partial least-squares, pairwise correlation, forward-and best subset selection methods for prediction of retention indices for aliphatic alcohols. J Chem Inf Model 2005; 45: 339-346.
[19] Subramanian A, Tamayo P, Mootha VK, Mukherjee S, Ebert BL, Gillette MA, Paulovich A, Pomeroy SL, Golub TR, Lander ES and Mesirov JP. Gene set enrichment analysis: a knowledge-based approach for interpreting genome-wide expression profiles. Proc Natl Acad Sci U S A 2005; 102: 15545-15550.
[20] Aran D, Hu Z and Butte AJ. xCell: digitally portraying the tissue cellular heterogeneity landscape. Genome Biol 2017; 18: 1-14.
[21] Shipley WU, Seiferheld W, Lukka HR, Major PP, Heney NM, Grignon DJ, Sartor O, Patel MP, Bahary JP and Zietman AL. Radiation with or without antiandrogen therapy in recurrent prostate cancer. N Engl J Med 2017; 376: 417-428.
[22] Kuo YZ, Fang WY, Huang CC, Tsai ST, Wang YC, Yang CL and Wu LW. Hyaluronan synthase 3 mediated oncogenic action through forming inter-regulation loop with tumor necrosis factor alpha in oral cancer. Oncotarget 2017; 8: 15563.
[23] Auvinen P, Rilla K, Tumelius R, Tammi M, Sironen R, Soini Y, Kosma VM, Mannermaa A, Viikari J and Tammi R. Hyaluronan synthases (HAS1-3) in stromal and malignant cells correlate with breast cancer grade and predict patient survival. Breast Cancer Res Treat 2014; 143: 277-286.
[24] Bai F, Jiu M, You Y, Feng Y, Xin R, Liu X, Mo L and Nie Y. miR-29a-3p represses proliferation and metastasis of gastric cancer cells via attenuating HAS3 levels. Mol Med Rep 2018; 17: 8145-8152.
[25] Teng BP, Heffler MD, Lai EC, Zhao YL, LeVea CM, Golubovskaya VM and Bullarddunn KM. Inhibition of hyaluronan synthase-3 decreases subcutaneous colon cancer growth by increasing apoptosis. Anticancer Agents Med Chem 2011; 11: 620-628.
[26] Chang IW, Liang PI, Li CC, Wu WJ, Huang CN, Lin VC, Hsu CT, He HL, Wu TF and Hung CH. HAS3 underexpression as an indicator of poor prognosis in patients with urothelial carcinoma of the upper urinary tract and urinary bladder. Tumour Biol 2015; 36: 5441-5450.
[27] Liu N, Gao F, Han Z, Xu X, Underhill CB and Zhang L. Hyaluronan synthase 3 overexpression promotes the growth of TSU prostate cancer cells. Cancer Res 2001; 61: 5207-5214.
[28] Czyrnik ED, Wiesehöfer M, Dankert JT and Wennemuth G. The regulation of HAS3 by miR-10b and miR-29a in neuroendocrine transdifferentiated LNCaP prostate cancer cells. Biochem Biophys Res Commun 2020; 523: 713-718.
[29] Wan Q, Tang J, Han Y and Wang D. Co-expression modules construction by WGCNA and identify potential prognostic markers of uveal melanoma. Exp Eye Res 2018; 166: 13-20.
[30] Feng Y, Ji D, Huang Y, Ji B, Zhang Y, Li J, Peng W, Zhang C, Zhang D and Sun Y. TGM3 functions as a tumor suppressor by repressing epithelial-to-mesenchymal transition and the PI3K/AKT signaling pathway in colorectal cancer. Oncol Rep 2020; 43: 864-876.
[31] Li W, Zhang Z, Zhao W and Han N. Transglutaminase 3 protein modulates human esopha-

geal cancer cell growth by targeting the NF-κB signaling pathway. Oncol Rep 2016; 36: 1723-1730.
[32] Wu X, Wang R, Jiao J, Li S, Yu J, Yin Z, Zhou L and Gong Z. Transglutaminase 3 contributes to malignant transformation of oral leukoplakia to cancer. Int J Biochem Cell Biol 2018; 104: 34-42.
[33] Hu JW, Yang ZF, Li J, Hu B, Luo CB, Zhu K, Dai Z, Cai JB, Zhan H, Hu ZQ, Hu J, Cao Y, Qiu SJ, Zhou J, Fan J and Huang XW. TGM3 promotes epithelial-mesenchymal transition and hepatocellular carcinogenesis and predicts poor prognosis for patients after curative resection. Dig Liver Dis 2020; 52: 668-676.
[34] Park WJ, Lee SE, Kwon NS, Baek KJ, Kim DS and Yun HY. Leucine-rich glioma inactivated 3 associates with syntaxin 1. Neurosci Lett 2008; 444: 240-244.
[35] Park WJ, Lim YY, Kwon NS, Baek KJ, Kim DS and Yun HY. Leucine-rich glioma inactivated 3 induces neurite outgrowth through Akt and focal adhesion kinase. Neurochem Res 2010; 35: 789-796.
[36] Kim DS, Kwon NS and Yun HY. Leucine rich repeat LGI family member 3: integrative analyses reveal its prognostic association with non-small cell lung cancer. Oncol Lett 2019; 18: 3388-3398.
[37] Kwon NS, Kim DS and Yun HY. Leucine-rich glioma inactivated 3: integrative analyses support its prognostic role in glioma. Onco Targets Ther 2017; 10: 2721.
[38] Zhang Z, Wang Q, Zhang M, Zhang W, Zhao L, Yang C, Wang B, Jiang K, Ye Y and Shen Z. Comprehensive analysis of the transcriptome-wide m6A methylome in colorectal cancer by MeRIP sequencing. Epigenetics 2021; 16: 425-435.
[39] Feng P, Ge Z, Guo Z, Lin L and Yu Q. A comprehensive analysis of the downregulation of miRNA-1827 and its prognostic significance by targeting SPTBN2 and BCL2L1 in ovarian cancer. Front Mol Biosci 2021; 8: 687576.
[40] Wen JX, Li XQ and Chang Y. Signature gene identification of cancer occurrence and pattern recognition. J Comput Biol 2018; 25: 907-916.
[41] Liu D, Chan SL, de Souza-Pinto NC, Slevin JR, Wersto RP, Zhan M, Mustafa K, de Cabo R and Mattson MP. Mitochondrial UCP4 mediates an adaptive shift in energy metabolism and increases the resistance of neurons to metabolic and oxidative stress. Neuromolecular Med 2006; 8: 389-413.
[42] Ramsden DB, Ho PW, Ho JW, Liu HF, So DH, Tse HM, Chan KH and Ho SL. Human neuronal uncoupling proteins 4 and 5 (UCP4 and UCP5): structural properties, regulation, and physiological role in protection against oxidative stress and mitochondrial dysfunction. Brain Behav 2012; 2: 468-478.
[43] Wu Q and Maniatis T. A striking organization of a large family of human neural cadherin-like cell adhesion genes. Cell 1999; 97: 779-790.
[44] Wende H, Volz A and Ziegler A. Extensive gene duplications and a large inversion characterize the human leukocyte receptor cluster. Immunogenetics 2000; 51: 703-713.
[45] Long G, Ouyang W, Zhang Y, Sun G, Gan J, Hu Z and Li H. Identification of a DNA repair gene signature and establishment of a prognostic nomogram predicting biochemical-recurrence-free survival of prostate cancer. Front Mol Biosci 2021; 8: 66.
[46] Lv D, Wu X, Chen X, Yang S, Chen W, Wang M, Liu Y, Gu D and Zeng G. A novel immune-related gene-based prognostic signature to predict biochemical recurrence in patients with prostate cancer after radical prostatectomy. Cancer Immunol Immunother 2021; 70: 3587-3602.
[47] Bancroft EK, Page EC, Castro E, Lilja H, Vickers A, Sjoberg D, Assel M, Foster CS, Mitchell G and Drew K. Targeted prostate cancer screening in BRCA1 and BRCA2 mutation carriers: results from the initial screening round of the IMPACT study. Eur Urol 2014; 66: 489-499.
[48] Petrovics G, Price DK, Lou H, Chen Y, Garland L, Bass S, Jones K, Kohaar I, Ali A and Ravindranath L. Increased frequency of germline BRCA2 mutations associates with prostate cancer metastasis in a racially diverse patient population. Prostate Cancer Prostatic Dis 2019; 22: 406-410.
[49] Cheng HH, Pritchard CC, Boyd T, Nelson PS and Montgomery B. Biallelic inactivation of BRCA2 in platinum-sensitive metastatic castration-resistant prostate cancer. Eur Urol 2016; 69: 992-995.
[50] Pomerantz MM, Spisák S, Jia L, Cronin AM, Csabai I, Ledet E, Sartor AO, Rainville I, O'Connor EP and Herbert ZT. The association between germline BRCA2 variants and sensitivity to platinum-based chemotherapy among men with metastatic prostate cancer. Cancer 2017; 123: 3532-3539.
[51] Mota JM, Barnett E, Nauseef JT, Nguyen B, Stopsack KH, Wibmer A, Flynn JR, Heller G, Danila DC and Rathkopf D. Platinum-based chemotherapy in metastatic prostate cancer with DNA repair gene alterations. JCO Precis Oncol 2020; 4: 355-366.
[52] de Bono J, Mateo J, Fizazi K, Saad F, Shore N, Sandhu S, Chi KN, Sartor O, Agarwal N and Olmos D. Olaparib for metastatic castration-resistant prostate cancer. N Engl J Med 2020; 382: 2091-2102.

Supplementary Table 1. List of the genes in three commercial panels for PCa risk-stratification

Test	Biomarkers	Genes	Ref
OncotypeDx	17 genes	*BGN, COL1A1, SFRP4, FLNC, GSN, TPM2, GSTM2, GAM13C, KLK2, AZGP1, SRD5A2, TPX2, ARF1, ATP5E, CLTC, GPS1, PGK1*	[1-3]
Decipher	22 genes	*LASP1, IQGAP3, NFIB, S1PR4, THBS2, ANO7, PCDH7, MYBPC1, EPPK1, TSBP, PBX1, NUSAP1, ZWILCH, UBE2C, CANK2N1, RABGAP1, PCAT-32, GLYATL1P4/ PCAT-80, TNFRSF19*	[4-7]
Prolaris	46 genes	*FOXM1, CDC20, CDKN3, CDC2, KIF11, KIAA0101, NUSAP1, CENPF, ASPM, BUB1B, RRM2, DLGAP5, BIRC5, KIF20A, PLK1, TOP2A, TK1, PBK, ASF1B, C18orf24, RAD54L, PTTG1, CDCA3, MCM10, PRC1, DTL, CEP55, RAD51, CENPM, CDCA8, ORC6L, RPL38, UBA52, PSMC1, RPL4, RPL37, RPS29, SLC25A3, CLTC, TXNL1, PSMA1, RPL8, MMADHC, RPL13A, LOC728658, PPP2CA, MRFAP1*	[8-12]

Supplementary Table 2. The AUC values of the 8-gene signature and three commercial panels for predicting 1-, 2- and 3-year BFS

Panel	1 year-AUC	*p* value	2 year-AUC	*p* value	3 year-AUC	*p* value
8-gene vs. Decipher	0.737 vs. 0.612	0.226	0.760 vs. 0.619	0.074	0.737 vs. 0.702	0.563
8-gene vs. OncotypeDx	0.737 vs. 0.712	0.776	0.760 vs. 0.698	0.347	0.737 vs. 0.761	0.651
8-gene vs. Prolaris	0.737 vs. 0.718	0.820	0.760 vs. 0.726	0.616	0.737 vs. 0.784	0.376

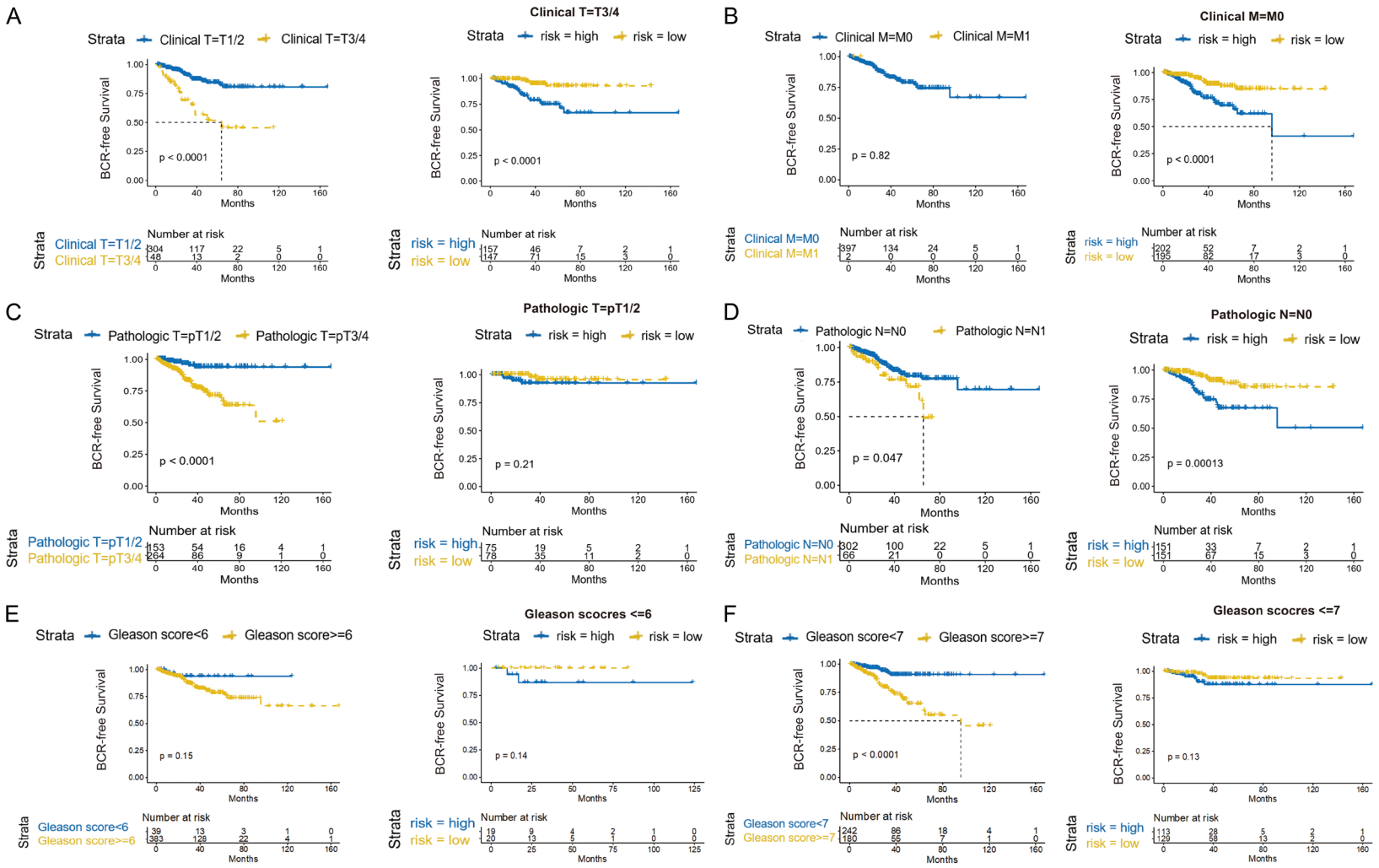

Supplementary Figure 1. Performance evaluation of the 8-gene signature in the subgroups stratified according to TNM status or Gleason score in the TCGA cohort. Kaplan-Meier BFS analyses of the 8-gene predicative model in the subgroup with clinical stage T1-2 PCa (A), clinical stage M0 PCa (B), pathologic stage T1-2 PCa (C), pathologic stage N0 PCa (D), or a Gleason score of ≤6 (E) or 7 (F). BFS: biochemical recurrence-free survival; TCGA: The Cancer Genome Atlas Project; PCa: prostate cancer.

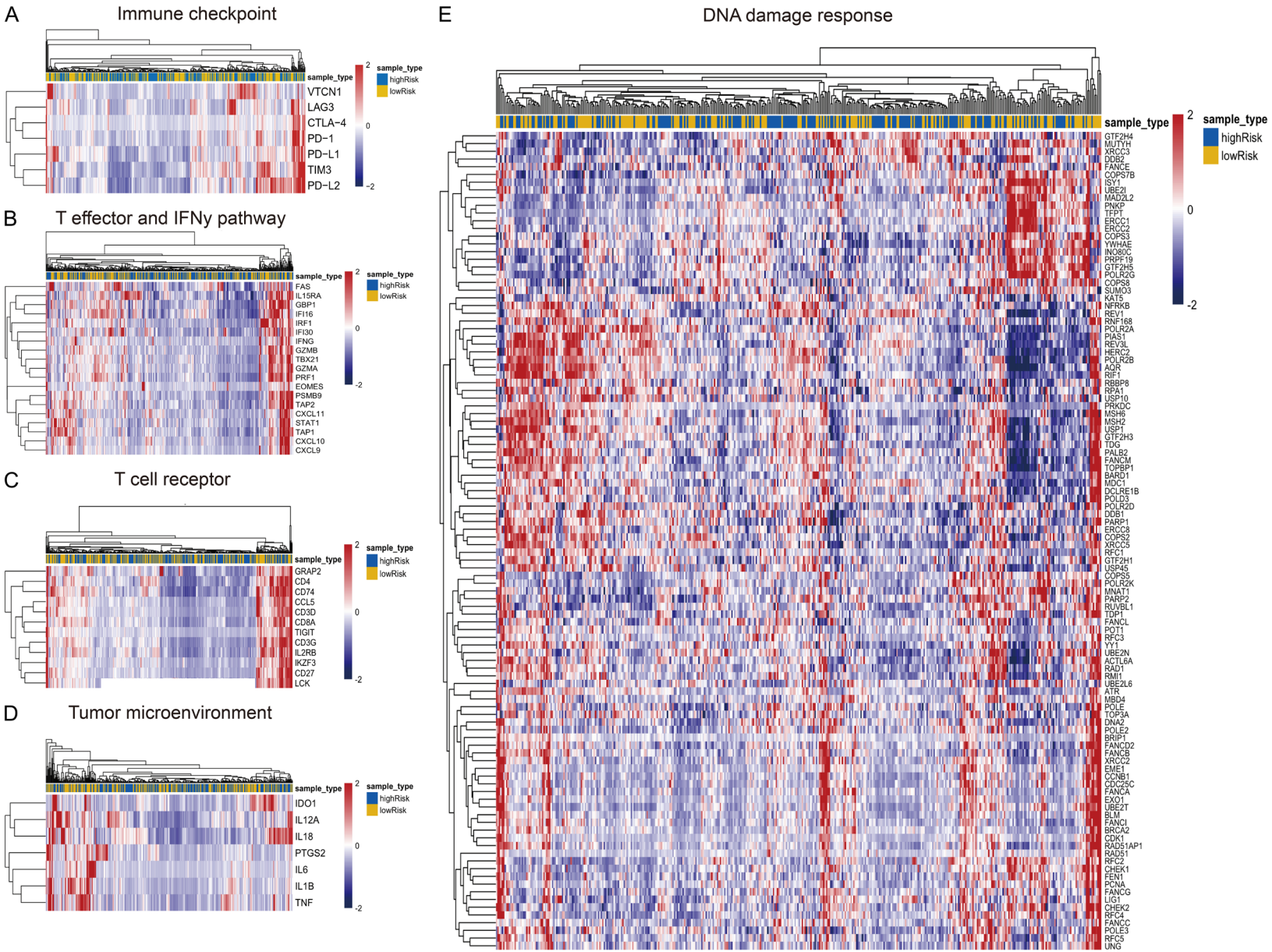
A
Immune checkpoint
sample_type
VTCN1
LAG3
CTLA−4
PD−1
PD−L1
TIM3
PD−L2
B
T effector and IFNy pathway
FAS
IL15RA
GBP1
IFI16
IRF1
IFI30
IFNG
GZMB
TBX21
GZMA
PRF1
EOMES
PSMB9
TAP2
CXCL11
STAT1
TAP1
CXCL10
CXCL9
C
T cell receptor
GRAP2
CD4
CD74
CCL5
CD3D
CD8A
TIGIT
CD3G
IL2RB
IKZF3
CD27
LCK
D
Tumor microenvironment
IDO1
IL12A
IL18
PTGS2
IL6
IL1B
TNF
highRisk
lowRisk
E
DNA damage response

Supplementary Figure 2. mRNA expression profiles of different gene classifications between high-risk and low-risk groups in the TCGA cohort. The heat maps show mRNA expression profiles of different gene classifications between high-risk and low-risk groups, including common immune checkpoints (A), representative genes of IFNγ pathway, effector T cell (B), T cell receptor (C), and the tumor microenvironment (D), and DNA damage repair genes (E). TCGA: The Cancer Genome Atlas Project.

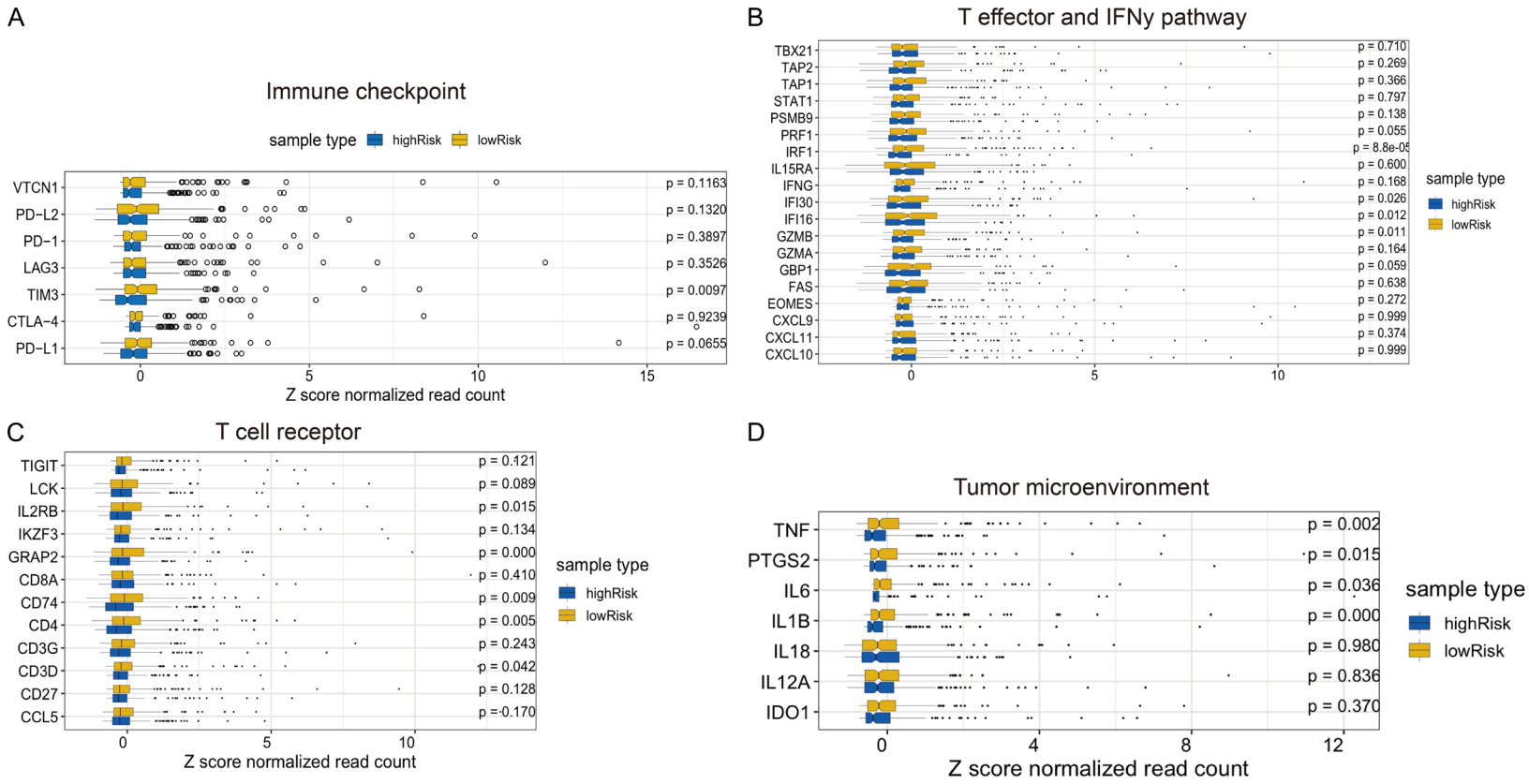

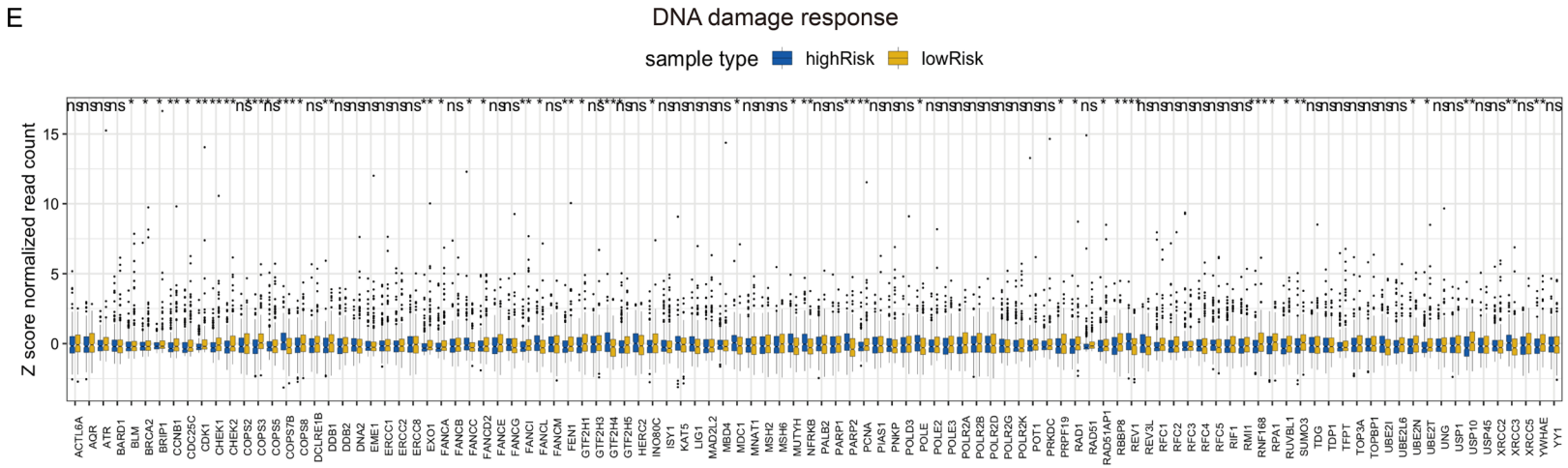

Supplementary Figure 3. Comparison of mRNA expression of different gene classifications between high-risk and low-risk groups in the TCGA cohort. The mRNA expression profiling analyses for common immune checkpoints (A), representative genes of IFNγ pathway, effector T cell (B), T cell receptor (C), and the tumor microenvironment (D), and DNA damage repair genes (E) between the two risk groups. *P<0.05, **P<0.01, ***P<0.001, and ****P<0.0001. TCGA: The Cancer Genome Atlas Project.

Supplementary Table 3. The differentially expressed DNA damage repair genes between the high-risk and low-risk groups in the TCGA cohort

Gene	*P* value	High-risk	Low-risk
BLM	0.029829042	-0.103942574	0.112135092
BRCA2	0.041661165	-0.097468548	0.105150798
BRIP1	0.019382566	-0.113383545	0.122320179
CCNB1	0.004667985	-0.134548703	0.145153527
CDC25C	0.030037404	-0.102600358	0.110687085
CDK1	0.005217301	-0.134560353	0.145166095
CHEK1	0.001822992	-0.148519804	0.160225799
CHEK2	0.001515887	-0.150122304	0.161954603
COPS3	1.22E-05	-0.205155828	0.221325745
COPS7B	0.000934291	0.154170673	-0.166322056
COPS8	0.024320428	-0.10586488	0.11420891
DDB1	0.005700649	-0.129984756	0.140229859
EXO1	0.004029355	-0.13711129	0.147918091
FANCA	0.028976696	-0.103627351	0.111795024
FANCC	0.013443946	0.113788324	-0.122756862
FANCD2	0.021192817	-0.10931184	0.117927551
FANCI	0.004434624	-0.135842843	0.146549669
FANCL	0.021431007	0.107706194	-0.116195352
FEN1	0.00713573	-0.127940837	0.138024844
GTF2H1	0.020075807	-0.109635925	0.11827718
GTF2H4	3.37E-06	0.214328168	-0.231221029
INO80C	0.017749556	-0.111841635	0.120656739
MDC1	0.042617574	0.095275714	-0.102785129
MUTYH	0.040772495	0.095478393	-0.103003784
NFRKB	0.002788265	0.138511415	-0.149428571
PARP2	0.00411484	0.134869937	-0.14550008
PCNA	0.002844698	-0.142599687	0.153839071
POLE	0.026184095	0.104749878	-0.113006026
PRPF19	0.029342079	-0.102880734	0.11098956
RAD1	0.046810852	-0.093702158	0.10108755
RAD51AP1	0.031127262	-0.102810912	0.110914235
RBBP8	0.024392086	-0.105786426	0.114124273
REV1	0.000253648	0.170397492	-0.183827837
RNF168	0.00072464	-0.158764688	0.171278161
RPA1	0.032319255	-0.100279107	0.108182879
RUVBL1	0.03174482	-0.101103648	0.109072408
SUMO3	0.005093212	-0.130476075	0.140759904
UBE2N	0.028733437	-0.103123008	0.11125093
UBE2T	0.026203703	-0.10546642	0.113779044
USP10	0.002250907	-0.142820558	0.154077351
XRCC3	0.005761013	0.129838086	-0.14007163
YWHAE	0.006637241	-0.127494558	0.13754339

References

[1] Cullen J, Rosner IL, Brand TC, Zhang N, Tsiatis AC, Moncur J, Ali A, Chen Y, Knezevic D, Maddala T, Lawrence HJ, Febbo PG, Srivastava S, Sesterhenn IA and McLeod DG. A biopsy-based 17-gene genomic prostate score predicts recurrence after radical prostatectomy and adverse surgical pathology in a racially diverse population of men with clinically low- and intermediate-risk prostate cancer. Eur Urol 2015; 68: 123-131.

[2] Van Den Eeden SK, Lu R, Zhang N, Quesenberry CP, Shan J, Han JS, Tsiatis AC, Leimpeter AD, Lawrence HJ, Febbo PG and Presti JC. A Biopsy-based 17-gene genomic prostate score as a predictor of metastases and prostate cancer death in surgically treated men with clinically localized disease. Eur Urol 2018; 73: 129-138.

[3] Klein EA, Yousefi K, Haddad Z, Choeurng V, Buerki C, Stephenson AJ, Li J, Kattan MW, Magi-Galluzzi C and Davicioni E. A genomic classifier improves prediction of metastatic disease within 5 years after surgery in node-negative high-risk prostate cancer patients managed by radical prostatectomy without adjuvant therapy. Eur Urol 2015; 67: 778-786.

[4] Karnes RJ, Choeurng V, Ross AE, Schaeffer EM, Klein EA, Freedland SJ, Erho N, Yousefi K, Takhar M, Davicioni E, Cooperberg MR and Trock BJ. Validation of a genomic risk classifier to predict prostate cancer-specific mortality in men with adverse pathologic features. Eur Urol 2018; 73: 168-175.

[5] Erho N, Crisan A, Vergara IA, Mitra AP, Ghadessi M, Buerki C, Bergstralh EJ, Kollmeyer T, Fink S, Haddad Z, Zimmermann B, Sierocinski T, Ballman KV, Triche TJ, Black PC, Karnes RJ, Klee G, Davicioni E and Jenkins RB. Discovery and validation of a prostate cancer genomic classifier that predicts early metastasis following radical prostatectomy. PLoS One 2013; 8: e66855.

[6] Ross AE, Feng FY, Ghadessi M, Erho N, Crisan A, Buerki C, Sundi D, Mitra AP, Vergara IA, Thompson DJ, Triche TJ, Davicioni E, Bergstralh EJ, Jenkins RB, Karnes RJ and Schaeffer EM. A genomic classifier predicting metastatic disease progression in men with biochemical recurrence after prostatectomy. Prostate Cancer Prostatic Dis 2014; 17: 64-69.

[7] Klein EA, Haddad Z, Yousefi K, Lam LL, Wang Q, Choeurng V, Palmer-Aronsten B, Buerki C, Davicioni E, Li J, Kattan MW, Stephenson AJ and Magi-Galluzzi C. Decipher genomic classifier measured on prostate biopsy predicts metastasis risk. Urology 2016; 90: 148-152.

[8] Canter DJ, Freedland S, Rajamani S, Latsis M, Variano M, Halat S, Tward J, Cohen T, Stone S, Schlomm T, Bishoff J and Bardot S. Analysis of the prognostic utility of the cell cycle progression (CCP) score generated from needle biopsy in men treated with definitive therapy. Prostate Cancer Prostatic Dis 2020; 23: 102-107.

[9] Cuzick J, Swanson GP, Fisher G, Brothman AR, Berney DM, Reid JE, Mesher D, Speights VO, Stankiewicz E, Foster CS, Møller H, Scardino P, Warren JD, Park J, Younus A, Flake DD, Wagner S, Gutin A, Lanchbury JS and Stone S. Prognostic value of an RNA expression signature derived from cell cycle proliferation genes in patients with prostate cancer: a retrospective study. Lancet Oncol 2011; 12: 245-255.

[10] Bishoff JT, Freedland SJ, Gerber L, Tennstedt P, Reid J, Welbourn W, Graefen M, Sangale Z, Tikishvili E, Park J, Younus A, Gutin A, Lanchbury JS, Sauter G, Brawer M, Stone S and Schlomm T. Prognostic utility of the cell cycle progression score generated from biopsy in men treated with prostatectomy. J Urol 2014; 192: 409-414.

[11] Freedland SJ, Choeurng V, Howard L, De Hoedt A, du Plessis M, Yousefi K, Lam LL, Buerki C, Ra S, Robbins B, Trabulsi EJ, Shah NL, Abdollah F, Feng FY, Davicioni E, Dicker AP, Karnes RJ and Den RB. Utilization of a genomic classifier for prediction of metastasis following salvage radiation therapy after radical prostatectomy. Eur Urol 2016; 70: 588-596.

[12] Cooperberg MR, Davicioni E, Crisan A, Jenkins RB, Ghadessi M and Karnes RJ. Combined value of validated clinical and genomic risk stratification tools for predicting prostate cancer mortality in a high-risk prostatectomy cohort. Eur Urol 2015; 67: 326-333.